ELSEVIER

Polymer 40 (1999) 2215–2229

polymer

Molecular rearrangements in ultra high molecular weight polyethylene after irradiation and long-term storage in air

V. Premnath[a], A. Bellare[b], E.W. Merrill[c,*], M. Jasty[d], W.H. Harris[d]

[a]*Department of Chemical Engineering and Program in Polymer Science and Technology, MIT, Cambridge, MA 02139, USA*
[b]*Department of Orthopedic Surgery, Brigham and Women's Hospital, Boston, MA 02115, USA*
[c]*Department of Chemical Engineering and Program in Polymer Science and Technology, MIT, Cambridge, MA 02139, USA*
[d]*Orthopedics Biomechanics Laboratory, Department of Orthopedic Surgery, Massachusetts General Hospital, Boston, MA 02114, USA*

Received 24 March 1998; revised 8 May 1998; accepted 15 May 1998

Abstract

Molecular rearrangements and alterations in supermolecular structure of ultra high molecular weight polyethylene (UHMWPE) due to cross-linking and oxidation-induced chain scission following irradiation and subsequent storage in air at room temperature have been studied over a period of 29 months. The techniques that were used are: equilibrium swelling in decalin, differential scanning calorimetry (DSC), small angle X-ray scattering (SAXS), Fourier transform infrared spectroscopy (FTIR) and electron spin resonance (ESR). The experimental results indicate that immediately after irradiation, cross-linking and an increase in crystallinity are the important processes. With time, chain scission induced by oxidation takes place resulting in a new phase of thinner crystallites in the amorphous region. In the absence of oxygen diffusion limitations, the free radicals survive for 30 months in the form of peroxides. The effect produced by higher doses and shorter aging times correspond to those produced by lower doses and longer aging times, thus, suggesting a superposition law between dose and aging time.

Keywords: Ultra high molecular weight polyethylene (UHMWPE); Radiation; Aging

1. Introduction

The effect of radiation on polyethylenes (chemistry, structure and properties), during and after irradiation, has been researched for the last 45 years and there are now several reviews on the subject [1–9]. The specific case of the effects of radiation on ultra high molecular weight polyethylene (UHMWPE), where the radiation induced changes are more dramatic than the other linear polyethylenes, has also been studied by several authors [10–28] of which the papers by Bhateja and co-workers [22–28] are most systematic at cataloging events for several doses and for a long period of time.

While there are several generalizations that can be made on the effect of radiation on polyethylenes, specific observations have differed between polyethylenes of different molecular weight [18,22–24], crystal morphology [3,7,8,25,28,29,30–33], additives [34–36], chain ends [3,37] etc. There are also differences in consequences depending on the temperature history [3,38], storage atmosphere before, during and after irradiation (for example, compare Refs. [39–44], sample sizes [29,44–47] etc.. Such variations and a lack of complete understanding of the underlying processes make it necessary to study the effects of radiation on polyethylene as a narrower problem after carefully defining an experimental system and parameters suitable for a particular application.

We have been interested in the specific case of post-irradiation oxidation of UHMWPE in total hip and knee replacement components sterilized by gamma irradiation before implantation. It has been known for several years that post-irradiation oxidation occurs in UHMWPE implants and results in increased crystallinity [10–28]. More recently, experimental observations on implants removed from patients during autopsy or revision surgery and those aged on the shelf for many years revealed a variation of the oxidation levels with depth [48–52]. This was explained to be the combined consequence of a variation of dose with depth and slow diffusion of oxygen into the implant [50] (a recent review describes the literature and process in greater detail [44]). The variation of oxidation

* Corresponding author.

0032-3861/99/$ - see front matter
PII: S0032-3861(98)00438-8

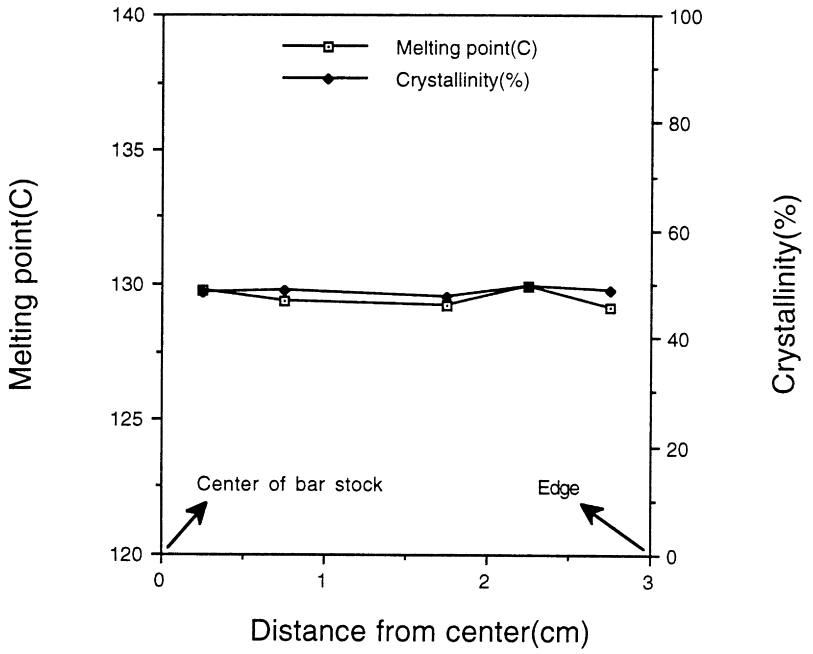

Fig. 1. Crystallinity at various radial positions on a GUR 415 bar stock.

with depth complicates the analysis of experimental results since one cannot differentiate between the effects of dose variation, the diffusion of oxygen and the reactions which cause the increase in crystallinity and chain scission. In this work, we studied the development of molecular and supermolecular structure of UHMWPE following irradiation in a system where: (a) the sample would have minimal dose variation with depth; and (b) the time scale of diffusion of oxygen to every part of the sample (approximately of the order of 1 day in our system) would be much smaller than the time scale of the long-term oxidation process (order of months). The advantage of such a system is that the experimental observations can be assumed to be a spatially uniform property of the sample. The method we use to accomplish this is the irradiation of a 1.6 mm thick UHMWPE sample with an electron beam[1] with certain precautions (see experimental section for more details) at an average dose rate of 20 kGy min^{-1} in air and at room temperature after which the sample is allowed to age for different times under the same conditions.

We examined the alterations of molecular and supermolecular structure of the UHMWPE sample prepared as described above over a period of 29 months using differential scanning calorimetry (DSC), small angle X-ray scattering (SAXS), swelling experiments, Fourier transform infrared spectroscopy (FTIR) and electron spin resonance (ESR). Similar experiments were performed by Bhateja and co-workers [22–28], but, this is the first study which combines all five of the above techniques for studying UHMWPE and which concerns itself with reducing spatial variation in properties.

[1] Electron irradiation produces substantially identical results as gamma radiation at the same absorbed energy per unit mass (i.e. dose), as measured by *G* values for stated processes, i.e. carbon-carbon scission. The dose rate being orders of magnitude lower for gamma irradiation, diffusion of oxygen into a sample under gamma irradiation could result in reactions not possible with high dose rate electron irradiation.

2. Experimental

2.1. Materials

The samples in this experiment were prepared from ram extruded UHMWPE bar stock (GUR 415, weight average molecular weight of approximately 6 million, obtained from Westlake Plastics Inc., Lenni, PA). Disks of diameter 30 mm and approximate thickness of 1.6 mm were machined out from the neighbouring regions of the same cylindrical bar stock. Neighbouring regions on the same bar stock were chosen because of concern over the variability in supermolecular structure and crystallinity between bar stocks of GUR 415 from different companies, between different lots from the same company and sometimes between samples from different locations on the same bar stock. Samples of dimensions approximately 3 cm × 1 cm × 0.16 cm were cut from these disks while avoiding the peripheral few millimeters of the disk. While the omission of the peripheral regions of the bar stock was fortuitous at the start of the experiment, it is specifically mentioned here because of reports [53] in literature of anisotropy of the supermolecular structure in the peripheral regions. In a separate experiment, it was verified that the crystallinity was uniform across the diameter of a typical GUR 415 rod stock from Westlake Plastics Inc. (Fig. 1).

2.2. Electron irradiation and aging

The samples were placed inside a pair (bottom and cover) of petri dishes of approximate thickness 1.7 mm each and irradiated in air with electrons of energy 2.5 MeV and a dose rate of 20 kGy min^{-1} (more accurately, 25 kGy $pass^{-1}$). The van de Graaff generator at the high voltage laboratory at M.I.T. was used for this purpose. It is known that electron (2.5 MeV) irradiation from this generator causes a distribution of doses with depth such that the first surface seen by the electrons gets a dose of approximately 60% of the peak dose which occurs at depths of 0.4–0.6 cm for a material of density 1 g cc^{-1}. The fact that the electrons pass through the 1.7 mm glass petri dish before striking the sample ensures that the 0.16 cm thick UHMWPE sample gets an approximately uniform dose throughout the sample at the peak dose (the electrons are incident on the 3 cm × 1 cm surface). Because the radiation was delivered in multiple passes, rather than continuously, the maximum temperature rise was no greater than 40°C above ambient. These specimens were then aged in air at room temperature for different times. Note that the oxygen diffusion times for the 0.16 cm thick sample is of the order of 1 day which is much smaller than the post-radiation aging times of several months. At the same time, 0.16 cm is thick enough to prevent any significant oxidation of the sample during irradiation (a maximum time period of 10 min). The samples which were studied for behaviour 'immediately after irradiation (0 months)' were tested within the first 5–10 hours. All experiments performed on samples aged '5 and 29 months' were performed within 20 days around the specified date, i.e. 5 months ± 10 days and 29 months ± 10 days.

2.3. Differential scanning calorimetry (DSC)

A Perkin–Elmer DSC7 was used with an ice-water heat sink and a heating and cooling rate of 10°C min^{-1} with a continuous nitrogen purge. All samples used weighed between 8–12 mg and an effort was made to prepare the pieces constituting the 8–12 mg of similar dimensions since the authors noticed a slight dependence on sample dimensions.

The mass fraction of crystalline regions (which we shall

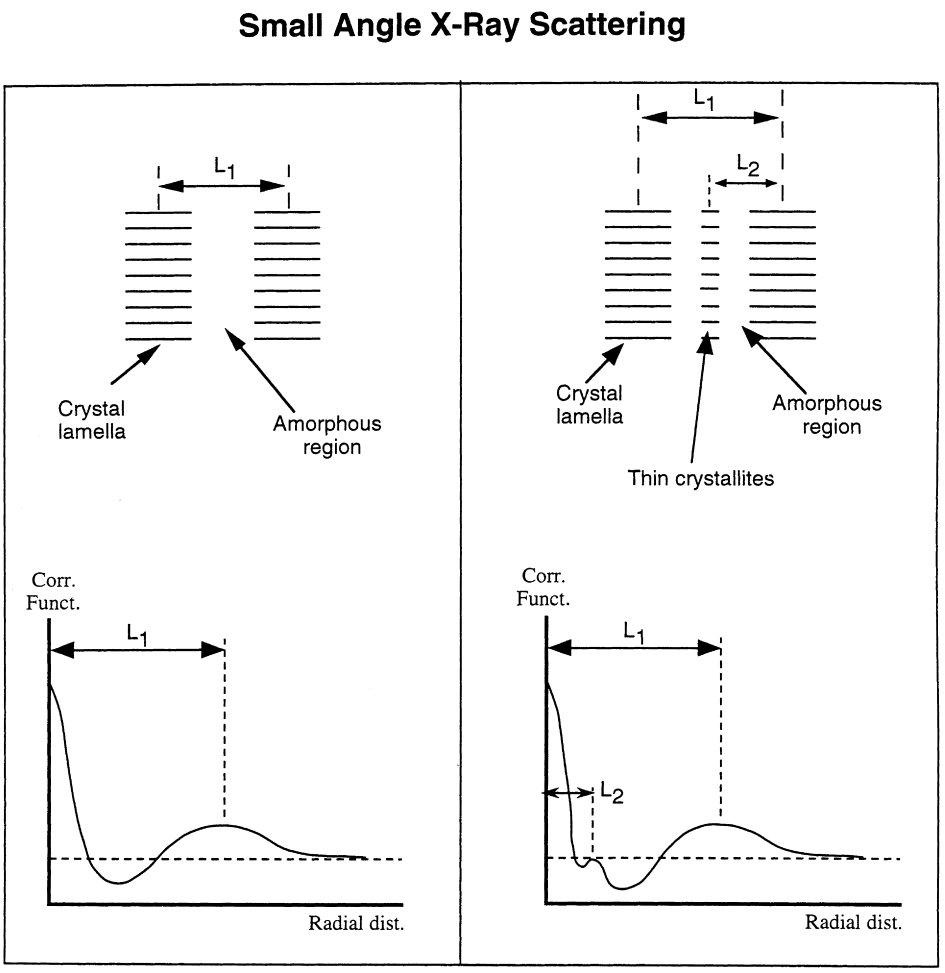

Fig. 2. Schematic showing the appearance of the correlation function curve for two crystal morphologies. The figure also shows the long period spacings corresponding to maxima on the correlation function curve.

call crystallinity, henceforth) in the samples were calculated using the following expression:

$$f_c = \frac{E}{m.\Delta H} \quad (1)$$

where, f_c is the crystallinity (mass fraction), E is the heat absorbed by the sample in melting (J), m is the mass of the sample (g) and ΔH is the heat of melting of polyethylene crystals ($\Delta H = 295\ \mathrm{J\ g^{-1}}$) [62]. The crystallinity measurement has an error of approximately ± 2%–3%.

2.4. Small angle X-ray scattering (SAXS)

A Rigaku rotating-anode Cu Ka X-ray source operating at 40 kV and 30 mA was used to perform the SAXS measurements. Data was obtained in the form of scattered X-ray intensities I (arbitrary units of counts per second) as a function of the scattering vector $\mathbf{q} = (4\pi/\lambda)\sin\theta$ (units of $\mathrm{nm^{-1}}$), where θ is half the scattering angle and λ is the wavelength of radiation (= 0.154 nm for Cu Kα). The X-ray beam from the point source was collimated using double-focusing Charles Supper mirrors. The beam profile was measured and used to desmear the scattering function. The beam diameter obtained from the full width at half-maximum (fwhm) of the beam profile corresponded to a q value of $0.006\ \mathrm{nm^{-1}}$. The scattered X-rays passed through a helium-filled tube to reduce background scattering and to increase the signal/noise ratio. A two-dimensional Siemens detector placed at a distance of 280 cm from the sample was used to detect the scattered X-rays between $\mathbf{q}_{min} = 0.06\ \mathrm{nm^{-1}}$ up to $\mathbf{q}_{max} = 0.7\ \mathrm{nm^{-1}}$. The detector was equipped with a position decoding circuit and controlled by a dedicated Nicolet computer. Data analysis was performed in a DOS-based personal computer using an ITP computer program developed by Glatter [54–56].

The SAXS correlation function curves obtained were used to determine: (a) the approximate long-period spacing from the position of the maximum; (b) an approximate measure of the size of the amorphous region from the slope of the linear section of the curve at small radial distances (the value of the x-axis at the intersection of the slope with the slope at the plateau is a measure equal to the number average thickness of the amorphous region [57]); and (c) the approximate distance between the edge of the larger crystal lamella to the far edge of the smaller crystallites from the radial distance at which the second maximum at smaller radial distances begins to appear (Bellare, A., unpublished results). Fig. 2 illustrates the above measurements for idealized systems. Exact calculations are not possible in this system because of the complicated correlation function obtained (the complication is due to a wide distribution of lamellar thicknesses [59]).

2.5. Swelling in decalin at 150°C

Samples of dimensions 1.5 mm × 1.5 mm × 1.5 mm were cut from the irradiated samples and submerged in decalin at 150°C for a period of 12–16 h. An antioxidant (1% *N*-phenyl-2-naphthylamine) was added to the decalin to prevent degradation of the sample. Both antioxidant and solvent were purchased from Aldrich Chemical Company

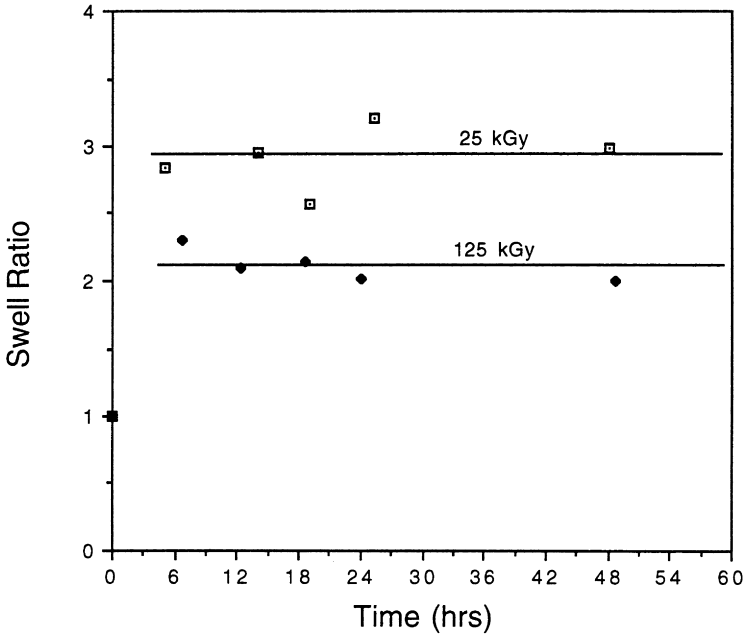

Fig. 3. Swell ratios measured at different times over a period of 48 h for the case of UHMWPE irradiated with doses of 2.5 MRad and 12.5 MRad. The figure illustrates the invariance of swell ratio during the swelling experiment. The extract percent is zero for both cases and throughout the experiment.

Inc., USA. Separate experiments (Fig. 3) on time-resolved swelling immediately after irradiation on samples (1.5 mm × 1.5 mm × 1.5 mm) which had received 25 and 125 kGy showed that: (a) equilibrium swelling is reached within the first 6 h; and (b) there is no measurable degradation of the sample in 48 h (since both extract percent and swell ratio remain constant). Three measurements were made on each sample: (1) the mass of the sample before the experiment (m_o, in mg); (2) mass of the swollen sample immediately after removing from swelling medium (m_s, in mg); and (3) the mass of the previously swollen sample after vacuum drying at 90°C for 12 h (m_d, in mg). All mass measurements were made using a Mettler AE 160 precision balance (accuracy 0.2 mg). Special precautions were necessary in the measurement of the swollen mass. The swollen sample was extracted quickly from the solvent, the solvent on the surface was wiped using lint-free tissue paper and the mass was measured immediately. This has to be done rapidly before any solvent within the sample evaporates and before the polyethylene starts crystallizing, thus, releasing the solvent by syneresis. The error in the measurement of the swollen mass increases as the swell ratio decreases.

The mass swell ratio ($\mathbf{q}_m$) and the extract percent (e) were calculated as follows:

$$q_m = \frac{m_s}{m_d} \tag{2}$$

$$e = 100\left(\frac{m_o - m_d}{m_o}\right) \tag{3}$$

Since the cross-linking process takes place heterogeneously with a preference for the amorphous region, the swell ratio data cannot be used to calculate the cross-linking density by using Flory's theory for swollen cross-linked networks.

2.6. Fourier transform infrared spectroscopy (FTIR)

FTIR was performed using a BioRad microscopic FTIR. Spectroscope in the transmission mode through rectangular sampling areas of dimensions 20 mm × 250 mm. This allowed sampling to be done at every 20 mm distance. A 50–100 mm thick film was microtomed across the 1.6 mm height of the aged sample. The microtoming was done from an area away from the edges of the aged sample. The sampling was done at various depths. The FTIR spectra was then used to calculate the oxidation index which was defined as follows:

$$\text{Oxidation Index} = \frac{A_{1650\ to\ 1800\text{cm}^{-1}}}{A_{1420\ to\ 1550\text{cm}^{-1}}} \tag{4}$$

where, $A_{1650\ to\ 1800\text{cm}^{-1}}$ is the absorbance of ketone, aldehyde, ester and carboxylic acid groups between 1650 and 1800 cm^{-1} and $A_{1420\ to\ 1550\text{cm}^{-1}}$ is the absorption corresponding to scissor motion of methyl and methylene groups (the concentration of which was assumed to be constant throughout the aging process).

2.7. Electron spin resonance (ESR)

ESR was performed using a Bruker ESP 300 EPR spectrometer. The measurement were done at room temperature on samples in ESR tubes purchased from Wilmad glass company, Buena, NJ. The measurement was done at 9.75 GHz (X-band) with the following typical settings: field centre, 3500 G; scan range, 300 G; scan time, 41 s; time constant, 1.28 s; modulation amplitude, 0.974 G. The incident microwave power was varied between 63 mW and 20 mW depending upon signal strength. Quantitative analysis was not performed. Our intention was to verify if radicals still existed after 29 months and if yes, to identify it.

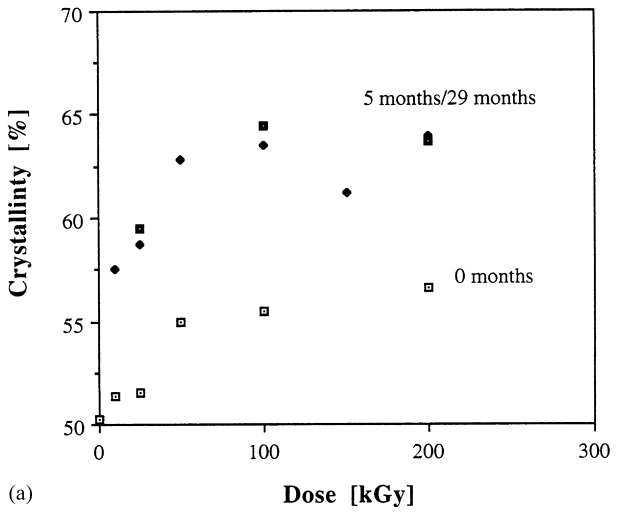

(a)

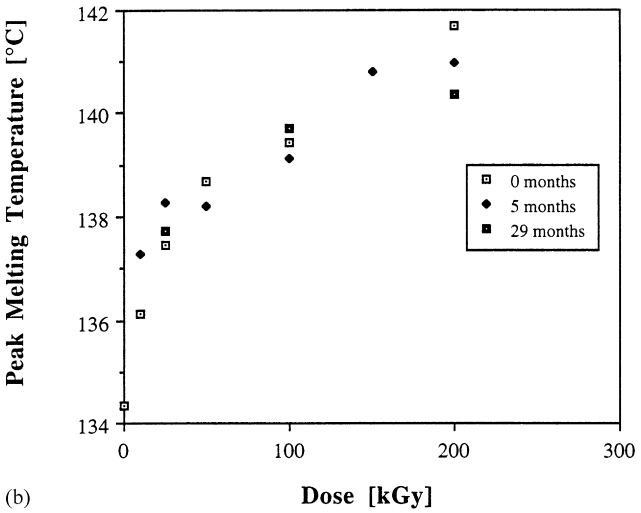

(b)

Fig. 4. Differential scanning calorimetry results: (a) Crystallinity variation with dose and time; (b) Variation of the peak melting temperature with dose and time. Symbols: (□) 0 months, (♦) 5 months, (■) 29 months.

3. Results and discussion

DSC and SAXS results give us information on the crystal morphology while the swelling experiments and FTIR spectroscopy give us information on oxidation induced chain scission and cross-linking. ESR indicates the existence and the form of free radicals. We employed the combination of the above five techniques to reveal the underlying processes.

3.1. Differential scanning calorimetry

The crystallinity of the samples for different radiation doses and at different times are shown in Fig. 4a. The crystallinity increased monotonically with dose immediately after irradiation but the increase was less rapid as the dose increased. More interestingly, the increase in crystallinity was substantial in the first 5 months after which there was no measurable increase in the crystallinity.

Fig. 4b is a plot of the peak melting temperature as a function of dose and time. The peak melting temperature increased with dose, but the change with time was negligibly small. The only noticeable change with time was for the 200 kGy sample, in which case there was a decrease in the melting point with increasing time. This is also clearly seen in Fig. 5. In addition, the melting temperatures were unusually high for polyethylene. The trends in Fig. 4a and b are consistent with that of Bhateja [24] though the magnitude of change is different especially at larger times. The differences could be due to the specific kind of UHMWPE used and processing history of the sample.

Fig. 5 shows the progression of the DSC curves with time for the sample case of 200 kGy dosage. The curves show the development of a shoulder in the DSC endotherm with time. Samples that received more than 50 kGy began to show a shoulder within 5 months. The shoulder became more prominent as time progressed. This shoulder was, however, not observed by Bhateja [24] for the corresponding time period.

3.2. Small angle X-ray scattering

Fig. 6 is a plot of SAXS correlation functions for 25 kGy (Fig. 6a) and 200 kGy (Fig. 6b). For the sample irradiated to a dose of 25 kGy, there were no noticeable changes in the long period spacing (corresponding to the position of the peak around 494 Å) or the size of the amorphous region (evaluated using the slope of the linear portion of the correlation function). There were also no secondary peaks. However, the correlation function of the 200 kGy samples showed several noticeable features: (a) The long period spacing decreased slightly with time; (b) the size of the

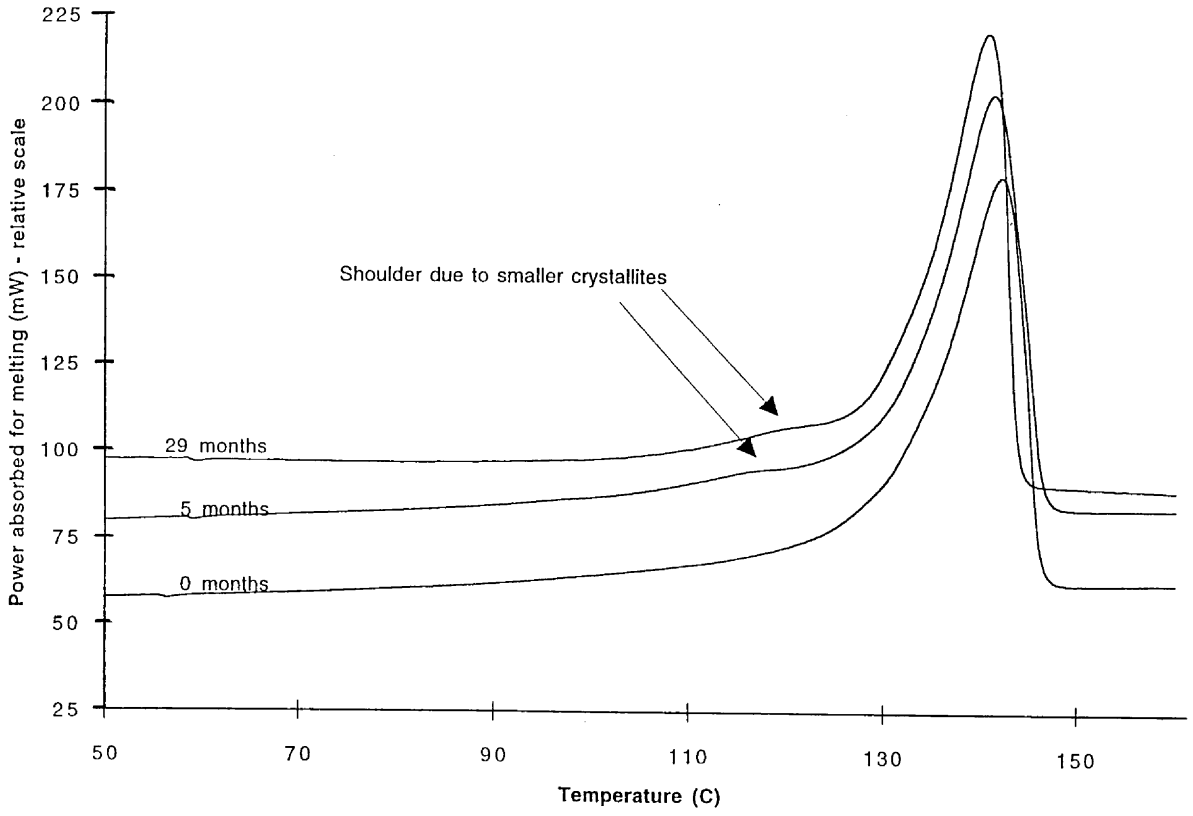

Fig. 5. Differential scanning calorimetry endotherms for different times. Dose was 200 kGy. The figure illustrates the development of a shoulder resulting from the creation of smaller crystallites.

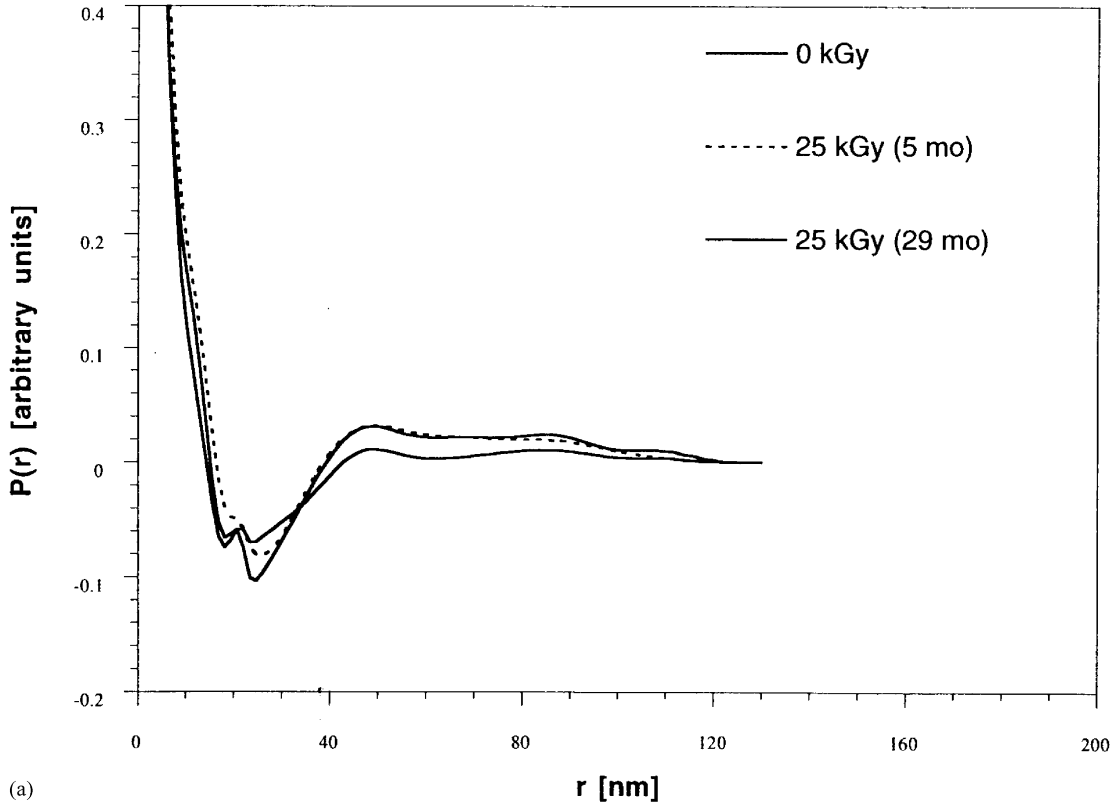

(a)

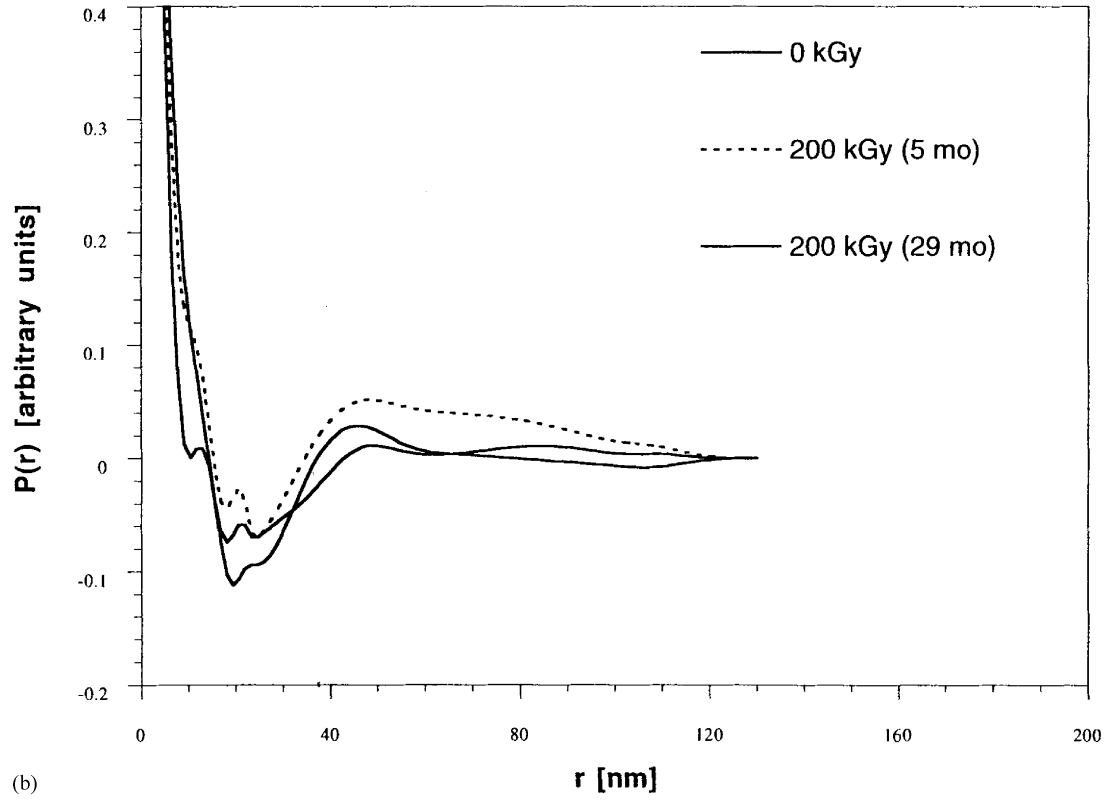

(b)

Fig. 6. SAXS correlation functions illustrating changes in morphology with time for:(a) 2.5 MRad; and (b) 20 MRad.

amorphous region decreased with time (the decrease was more rapid in the first 5 months); (c) distortions in the curve appeared which are precursors to peaks corresponding to new spacings resulting from the creation of smaller crystallites in the amorphous regions (at radial distance = 130 Å). Fig. 7 is a plot of the SAXS correlation functions for various doses at 29 months. The size of the amorphous region decreased with dose. It is also clear that at 29 months, the 25 kGy sample did not have smaller crystallites (at radial distance = 130 Å) but the samples that received larger doses (100 and 200 kGy) did. Immediately after irradiation, there were no significant changes in the thickness of the amorphous region.

While the SAXS correlation function curves are not amenable to exact calculation, an approximate calculation to obtain orders of magnitude and relative variation of dimensions is possible (with the assistance of DSC results). Our calculations indicated the following: The starting material had a long spacing of approximately 490 Å. If the weight percent of the crystalline fraction was 52%, then the amorphous region was 255 Å thick. After 29 months, the percent crystallinity for the sample that received the highest dose studied (200 kGy) was 65% while the long period spacing was 455–468 Å. The second peak started appearing at 130 Å which gives the size of the smaller crystallites in the 20 MRad sample after 29 months to be approximately 50–60 Å.

3.3. Discussion of the DSC and SAXS results

3.3.1. Immediately after irradiation

We observed that there was an increase in the crystallinity (more accurately, the heat of fusion per gram of material) and the peak melting point (which is unusually high) while there were no significant changes in the thickness of the amorphous region. Further, there was no shoulder in the DSC endotherm immediately after irradiation even for large doses. Also there was no indication of smaller crystallites immediately after irradiation in the SAXS correlation function plots. This leads us to the hypothesis that in the absence of smaller crystallites, the increase in percent crystallinity must have been caused by fine rearrangements in the lamellae or at the crystal-amorphous interface (as speculated by Bhateja et al. [27]). The rearrangements probably follow radiation-induced non-oxidative backbone chain scission of chains at the mechanically strained entanglements [16]. The unusually high peak melting temperatures after irradiation suggest that the melting process is being kinetically arrested by the cross-links, thus, producing artifactually higher melting temperatures at the relatively fast heating rate of 10°C min^{-1}. Hence, it is likely that some fraction of the increase in the peak melting point is caused by the cross-links. This is further supported by the decrease in the peak melting point with time for the 200 kGy sample as aging causes chain scission and increased mobility of the chains.

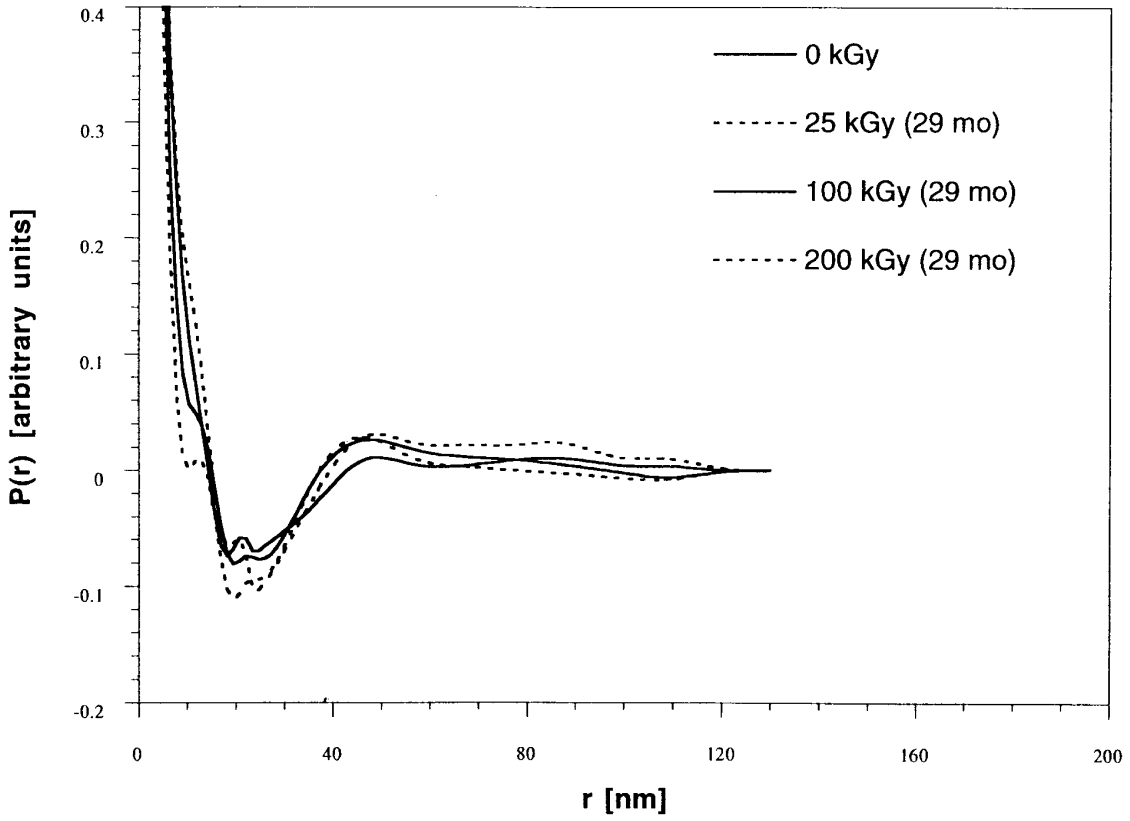

Fig. 7. SAXS correlation functions illustrating differences in morphology for UHMWPE samples aged for 29 months in air as a function of dosage.

3.3.2. In the next 5 months

We observed that the crystallinity increased significantly while the peak melting point did not change very much except at the larger doses where it decreased. Smaller crystallites developed in the samples irradiated to higher doses (DSC and SAXS). The thickness of the amorphous region also decreased. There was a small decrease in the long period too. These observations indicate that during this period the major change is the development of the smaller crystallites in the amorphous regions. These new crystallites explain the increase in crystallinity. Further, the fact that these crystallites can form indicates that some amount of chain scission has occurred which has freed the chains to move and recrystallize. This newly created freedom especially at the larger doses is probably the reason for the decrease in melting point. The creation of a denser phase (which occupies less volume) of thin crystallites in the amorphous regions probably also causes a shrinkage in the size of the amorphous region and long period spacing.

3.3.3. Between 5 months and 29 months

The same processes as that in the first 5 months occurred between 5 and 29 months, albeit at a much slower pace. This explains the remaining observations satisfactorily.

3.4. Swelling experiments

The extractable percent is the fraction of the polymer sample which is in the form of shorter, single chains unconnected to the network. The swell ratio gives an inverse

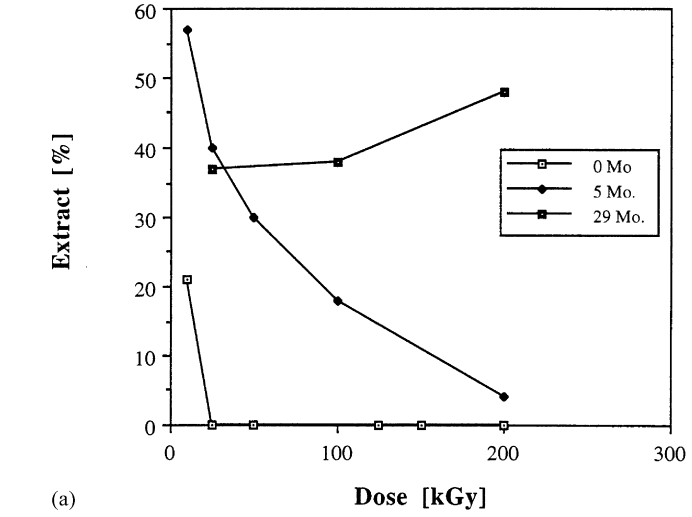

(a)

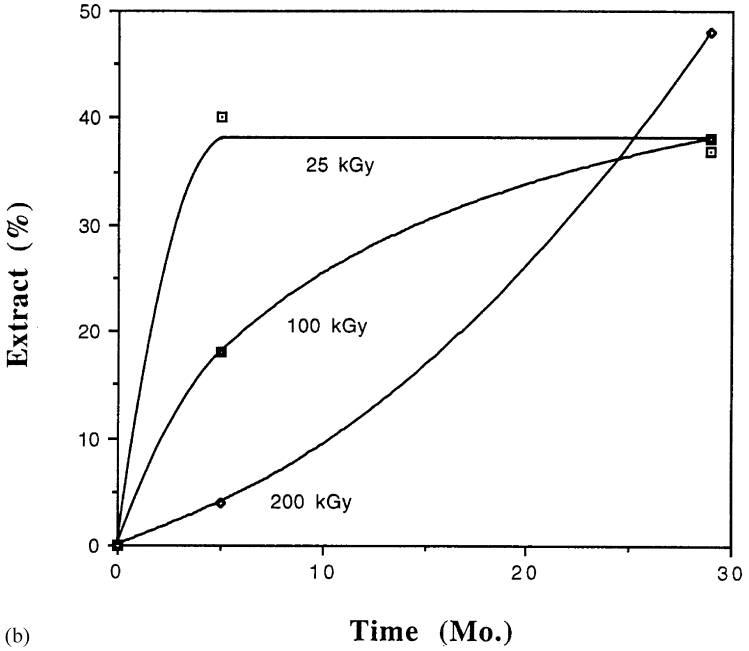

(b)

Fig. 8. Extract percent in swelling experiments: (a) Variation with dosage; (b) Variation with aging time. Non sterile 'control' is not included since it completely dissolved, i.e. extract % = 100.

measure of how tightly cross-linked the sample is, or more exactly an inverse measure of the concentration of elastically effective chains.

Fig. 8a plots the extractable percent as a function of dosage whereas Fig. 8b plots the extract percent as a function of time. As measured immediately after irradiation, the percent extractable had been reduced to zero at some dose equal to, or greater than 25 kGy. Over the first 5 months, we observed that the extractable percent increased as a function of time for all dosages (Fig. 8b) as a consequence of oxidation induced chain scission. While oxidation was highest where there were the largest number of available radicals (i.e. at higher doses), the number of cross-links were also the highest in the samples with higher doses.

Between 5 and 29 months, we observed that the extractable percent for the 25 kGy sample did not increase measurably. In the same period, the extractable percent of the larger doses increased very quickly. These observations can be explained as follows: The behaviour shown by the 25 kGy sample was caused by the decrease in free radical concentration with time as a result of termination reactions. Once the concentration of radicals decreased, the rate of

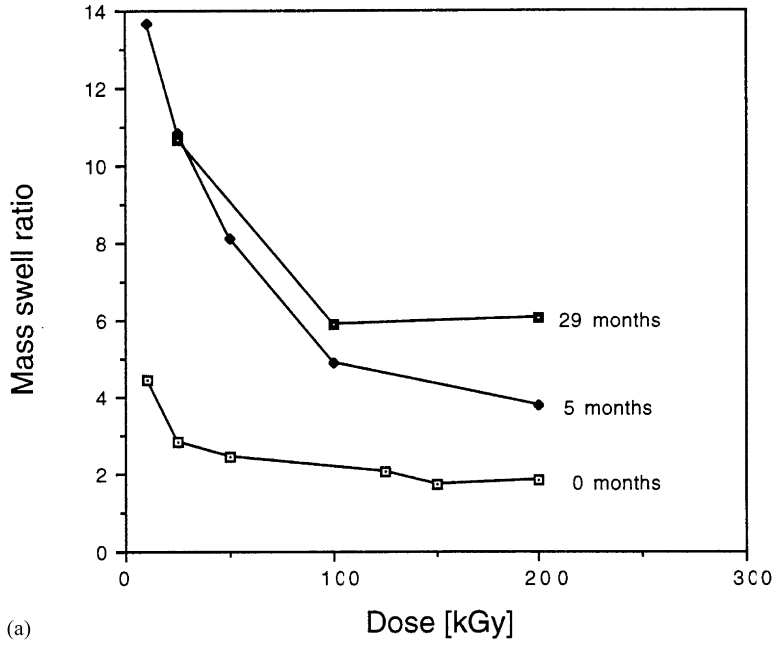

(a)

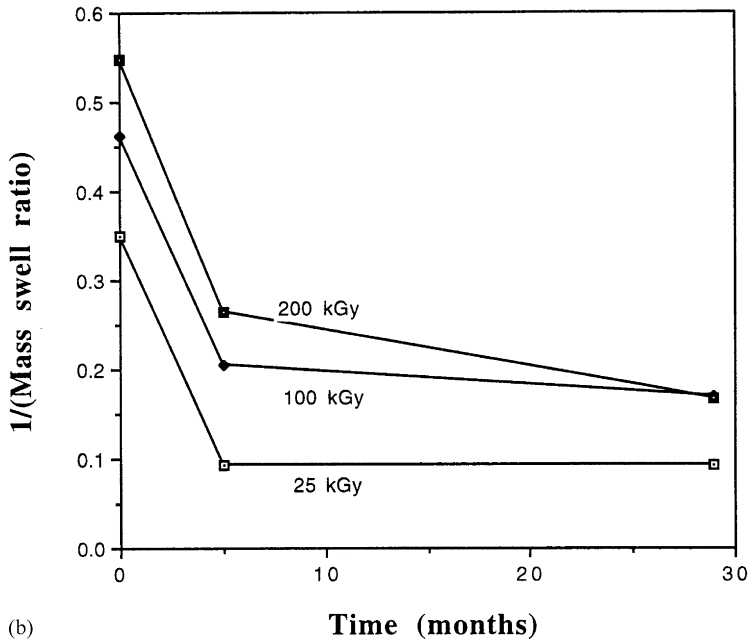

(b)

Fig. 9. Mass swell ratio from swelling experiments: (a) Variation of swell ratio with dosage; (b) Variation of the inverse of the swell ratio with aging time. The datapoint in Fig. 9b corresponding to 10 MRad and 5 months was obtained by interpolation using the data in Fig. 9a. Non sterile 'control' is not included since it completely dissolved (infinite swell ratio).

chain scission also decreased. In the case of the higher doses, oxidation induced chain scission in the first 5 months caused scission of chains and loosening of the network but did not produce small molecules which could be extracted. However, after 5 months the network became sufficiently loose and further chain scission produced larger extract percentages. Since samples that receive larger doses have higher free radical concentration (see for example Ref. [60]), the absolute radical concentration in these samples is higher for a longer period of time. Thus, oxidation-induced chain scission continues for a longer period of time in samples that received higher doses.

It is interesting to note that for the 25 kGy sample (which is relevant to the sterilization industry), the polymer is completely cross-linked with no extractable fraction immediately after irradiation. However, after just 5 months the extractable percent has gone up to 40%. Following this, the increase (if any) is very slow. Larger doses will result in less cross-linked materials only after 25–30 months (for the case of negligible oxygen diffusion limitations). Smaller doses on the other hand would mean that: (a) the polymer immediately after irradiation is not completely cross-linked into a network; and (b) in a few months, say, 5 months, the extractable percent of the polymer will be very high. This may be a concern if cross-linking is important for increased wear resistance.

The swell ratio of the polymer samples are plotted in Fig. 9a function of dose. Immediately after irradiation, the swell ratio was less than four for all doses (10–200 kGy) studied. An increase in dosage did not result in a substantial decrease in the swell ratio. The swell ratio increases substantially in the next 5 months, thus, indicating that the chains have become more mobile resulting from chain scission. The samples exposed to lower doses show a higher increase in swell ratio caused by a lesser number of cross-links that were present in them immediately after irradiation. In between 5 and 29 months, the increase in swell ratio for the samples that received smaller doses asymptotically levels to a steady value as the free radical concentration decreases. On the other hand, the increase in swell ratio continues for the higher dose samples albeit at a slower rate.

Fig. 9b is a plot of the inverse of the swell ratio as a function of time. An interesting feature to note is the similarity in general trends between Fig. 9a and b. This observation forces one to wonder if there exists a super-position law between dose and aging time. If so, dose variation could be used as way to do accelerated aging tests. It can also be shown that the plots of extract percent and crystallinity with dose would show similar variation as the plots of the inverse of extract percent and crystallinity with time, respectively. However, a more extensive study is required to confirm or reject this speculation. If it is true one would also have to determine the range of validity and the exact nature of the superposition law.

3.5. Fourier transform infrared spectroscopy (FTIR)

As discussed before, we decided to use electron irradiation hoping that the dose would be uniform throughout the sample. If this were true, one would expect the oxidation to be approximately uniform over the time scales studied since the order of magnitude of the diffusion time is only 1 day (much less than the time scale of months being investigated in this study). We decided to verify if this was indeed so. Fig. 10 is a plot of the variation of the oxidation index with

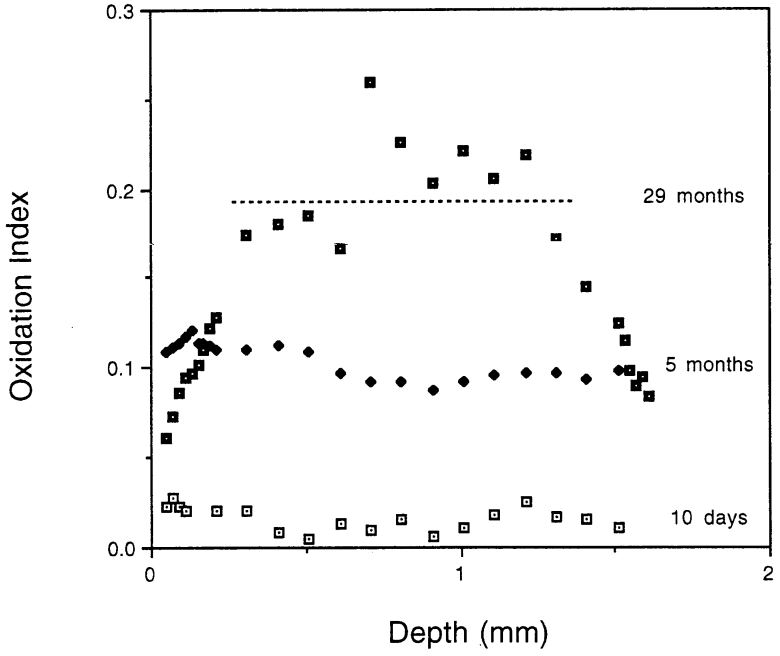

Fig. 10. A representative plot of oxidation index versus depth of the sample. These samples were all irradiated to 20 MRad and aged for different times.

depth in the sample for the case of 200 kGy. The oxidation was uniform for the 5 month old sample but was not so for the 29 month old sample. An approximately 200 μm thick surface layer had lower oxidation levels than the bulk which had an approximately constant level of oxidation. Other 29-month-old samples exposed to different doses showed similar behaviour. This surface layer cannot be caused by a dose build-up as observed in gamma irradiation since the thickness of the surface layer is too small. Hence, we surmise that this is an artifact resulting from either a small difference in surface preparation of all the samples aged for 29 months (which we could not identify) or small differences in dose caused by scatter at the polymer-air interface which show up only when these differences are exaggerated by extensive oxidation.

Since 75% of the sample (the central core region) is uniformly oxidized, we decided to neglect this profile in our analysis. Fig. 11a and b plot the spatially averaged oxidation index as a function of dose and time. The oxidation was almost linear with dose at all times whereas incremental oxidation was higher at smaller times than at larger times. These trends are indicative of a diffusion and/or reaction process. The oxidation index varies roughly linearly with dose because the concentration of free radicals varies linearly with dose. The decrease of the oxidation rate with time could be caused by: (a) diffusion of the radicals along crystal stalks to the amorphous region; and/or (b) diffusion of oxygen from the amorphous regions to the radical in the crystalline region; and/or (c) *n*th order reaction kinetics of the various oxidation reactions (in which the rate equation is such that the rate of creation of a species depends on the product of '*n*' concentrations). The observed trend in

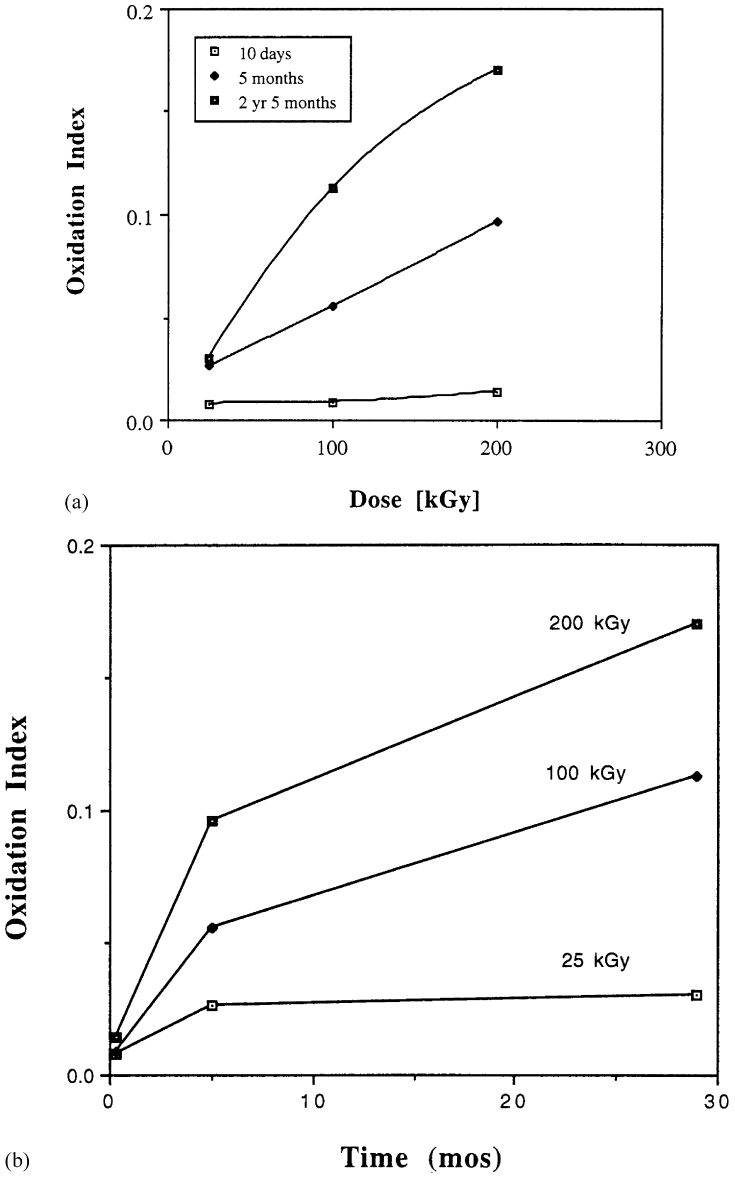

Fig. 11. Variation of the average oxidation index with: (a) dosage; and (b) aging time.

Table 1
Summary of ESR results

Dose	1 day	48 days	5/6 months	29/30 months	
Decreasing signal strength →					Increasing signal strength ↓
25 kGy	Sextet (alkyl)	Singlet (peroxy)	Singlet (peroxy)	Singlet (peroxy)	
200 kGy	—	—	Singlet (peroxy)	Singlet (peroxy)	

the oxidation versus time can result if any one or more of the above three processes were rate determining.

3.6. Electron spin resonance (ESR)

We performed ESR on our samples only to verify if the radicals still existed and to try and identify them. Table 1 is a summary of our results. In the 25 kGy sample, we observed a sextet signal corresponding to the alkyl radical after 1 day. For longer periods we observed a singlet signal corresponding to peroxides of the alkyl or allyl radical[2]. Our observation is consistent with that of Oonishi et al. [61] who observed similar spectra for doses of the order of magnitude of 10 kGy although they did not pursue the process beyond a few months. Peroxy radicals exist as long as 30 months. The fact that only peroxy radicals are seen at 48 days and 30 months seems to indicate that the radicals survive in this form in our system where oxygen diffusion is not the rate limiting process. This also implies that oxygen and most radicals in the sample manage to reach each other within the first 48 days. If that is so, it is the rate of the reactions converting peroxy radicals to the various oxidation products (ketones, aldehydes and alcohols) and not any of the diffusion processes which is rate determining for long-term aging (over a period of years).

4. Conclusions

Some aspects of the development of molecular and supermolecular structure of UHMWPE following irradiation in air were studied in this work using DSC, SAXS, swelling in a solvent, FTIR and ESR. The sequence of events which we conclude from our results are as follows.

1. *Immediately after irradiation*: the percent crystallinity increases with absorbed dose. This is probably caused by readjustment of chains at the crystal-amorphous interface following back bone chain scission of molecules in that region. There could also be some increase in the crystallinity resulting from perfection of the crystal following chain scission. The melting point as measured by DSC increases because of the arresting of the crystals during melting by the cross-links created during irradiation. For the doses studied here (10–200 kGy) and the experimental conditions, the effect of cross-linking exceeds the effect of chain scission. The degree of cross-linking is higher for higher doses. Oxidation during irradiation is negligible for our experimental system.
2. *In the first 5 months*: the oxidation rate is high during the first few months and increases linearly with the initially absorbed dose. The oxidation results in substantial chain scission. The degree of cross-linking decreases and small chains are generated which are extracted out of the network during swelling experiments. Thin crystallites are formed in the amorphous region because of the rearrangement of chains in the amorphous region. These chains have greater freedom than the chains in the amorphous region before oxidation-induced chain scission and are, hence, able to fit into crystals. The formation of these crystallites causes an increase in the fraction crystallinity. The long period spacing also shrinks following densification resulting from the formation of newer crystallites. The extent of chain scission is large enough at high doses to cause a reduction in the melting point by permitting the lamellae to melt more easily unrestricted by the too many cross-links. The fact that the chain scission reduces connections between lamellae is the likely reason for the brittleness that accompanies post-irradiation oxidation.
3. *Between 5 and 30 months*: the oxidation rate is much slower but its effect on the creation of small molecules is large especially for larger doses as indicated by the fast increase in the extractable percent. ESR results indicate that it is the oxidation reaction rate which is rate determining at these large times. It was also discovered that in the presence of oxygen, radicals survive in the form of peroxides for as long as 30 months. The chain scission continues at a lower rate increasingly disconnecting lamellae from one another. The swell ratio increases slowly with time as the population of elastically effective chains (connected at both ends to junctions) is decreased as a consequence of scission. The thin crystallites grow slowly and/or are perfected during this time period. The crystallinity increase is much lower than in the initial stages.

The following are some other conclusions of practical interest.

1. The removal of dose variation with depth and large oxygen diffusion times helps in understanding the

[2] Alkyl radicals are of the form -CH_2CH-CH_2- and the corresponding peroxides are of the form -CH_2-C(OO)H-CH_2-. Allyl are of the form -CH-CH=CH- and the corresponding peroxides are of the form -C(OO)H-CH=CH-.

aging process better. If these complications are not eliminated, results can be difficult to interpret as indicated by the strong dependence of the process on the dose observed in our study. There are two ways to achieve this: one is the method used in this study while the other method is to use gamma sterilization on a thicker sample and then discard an approximately 3 mm thick layer from the surface before aging.

2. The large variations in extract percent, swell ratio and crystallinity for the 25 kGy (which is the dose used by the sterilization industry) sample within the first 5 months indicates that significant changes take place while the implant is on the shelf. If one assumes that there are changes in the rate and/or mechanism of oxidation after the implant is inserted into the human body (perhaps resulting from a change in the oxidant concentration), then differences in shelf life between various implants will cause significant differences in their performance in vivo.
3. Our observation that there seems to be a superposition law between dose and aging time may be very useful for accelerated aging of UHMWPE samples.

Acknowledgements

VP would like to thank Mr. K. Wright of the High Voltage Research Lab for irradiating the samples and the discussions on irradiation, Mr. A. Modestino of the Chemical Engineering Dept, MIT, for assistance with ESR and Dr. O. Muratoglu of Massachusetts General Hospital for his loan of a computer program to oxidation indices from FTIR spectra. MRSEC shared facilities supported by the NSF under award number DMR-9400334 were used for some part of this work. The authors also wish to thank Prof. R.E. Cohen of the Department of Chemical Engineering, MIT, for allowing them to use his SAXS facility. This work was funded by the William H. Harris Foundation.

References

[1] Chapiro A. Radiation chemistry of polymeric systems. New York: Interscience, 1962.
[2] Dole M. Mechanism of chemical effects in irradiated polymers. In: Raff RAV, Doak KW, editors. Crystalline olefin polymers, vol. 1. New York: Interscience, 1965:845.
[3] Mandelkern L. In: Dole M, editor. The radiation chemistry of macromolecules. New York: Academic Press, 1972:287.
[4] Dole M. Oxidation of irradiated polymers. In: Dole M, editor. The radiation chemistry of macromolecules, vol. 2. New York: Academic Press, 1973:13.
[5] Wilson JE. Radiation chemistry of monomers. Polymers, and plastics. New York: Marcel Dekker, 1974.
[6] Makhlis FA. Radiation physics and chemistry of polymers. New York: Wiley, 1975.
[7] Dole M. Polym Plast Technol Engng 1979;13 (1):41.
[8] Keller A. Radiation effects and crystallinity in polyethylene and paraffins. In: Bassett DC, editor. Developments in crystalline polymers, vol. 1. London: Applied Science, 1982:37.
[9] Mukherjee AK, Gupta BD, Sharma PKJ. Macromol Sci Rev Macromol Chem Phys 1986;C26 (3):415.
[10] Brenner W, Adler A, Oswald HJ, Turi EA. J Appl Polym Sci 1969;13:2689.
[11] Nusbaum HJ, Rose RM. J Biomed Mater Res 1979;13:557.
[12] Lue CT, Ellis EJ, Crugnola A. Effects of gamma-irradiation on ultra-high-molecular-weight polyethylene. In: 39 Annual Conference of The Society of Plastics Engineers, SPE 1981:246.
[13] Roe RJ, Grood ES, Shastri R, Gosselin CA, Noyes FR. J Biomed Mater Res 1981;15:209.
[14] Grood ES, Shastri R, Hopson CN. J Biomed Mater Res 1982;16:399.
[15] Eyerer P, Ke YC. J Biomed Mater Res 1984;18:1137.
[16] Kamel I, Finegold L. Radiat Phys Chem 1985;26 (6):685.
[17] Streicher RM. Radiat Phys Chem 1988;31 (4) 5 6:693.
[18] Minkova L. Colloid Polym. Sci (Vol. 6–10) 1988:266.
[19] Kurth M, Eyerer P. Effects of radiation sterilization on UHMW-PE. In: Willert H-G, Buchhorn GH, Eyerer P, editors. Ultra-high molecular weight polyethylene as biomaterial in orthopedic surgery. Toronto: Hogrefe and Huber, 1991:82.
[20] Rimnac CM, Burstein AH, Carr JM, Klein RW, Wright TM, Butts FJ. Appl Biomater 1994;5:17.
[21] Rimnac CM, Klein RW, Betts F, Wright TM. J Bone Joint Surg 1994;76A (7):1052.
[22] Bhateja SK. Polymer 1982;23:654.
[23] Bhateja SK, Andrews EH, Young RJ. J Polym Sci, Polym Phys Ed 1983;21:523.
[24] Bhateja SK. J Appl Polym Sci 1983;28:861.
[25] Bhateja SK. J Macromol Sci -Phys 1983;B22 (1):159.
[26] Bhateja SK, Andrews EH. J Mater Sci 1985;20:2839.
[27] Bhateja SK, Andrews EH, Yarbrough SM. Polym J 1989;21 (9):739.
[28] Bhateja SK, Yarbrough SM, Andrews EH. J Macromol Sci Phys 1990;B29 (1):1.
[29] Dole M, Patel VM. Radiat Phys Chem 1977;9:433.
[30] Hikmet R, Keller A. Radiat Phys Chem 1987;29 (4):275.
[31] Hikmet R, Keller A. Radiat Phys Chem 1987;29 (1):15.
[32] Akay G, Cimen F, Tincer T. Radiat Phys Chem 1990;36 (3):337.
[33] Izumi Y, Nishii M, Seguchi T, Ema K, Yamamoto T. Radiat Phys Chem 1991;37 (2):213.
[34] Tsuji K. J Polym Sci Polym Lett 1973;11:351.
[35] Noakovic LJ, Gal O. Polym Degrad Stab 1995;50:53.
[36] Swartz D, Gsell R, King R, Devanathan D, Wallace S, Lin S, Rohr W. Aging of calcium stearate-free polyethylene. In: Transactions of the Fifth Biomaterials Congress, 29 May–2 June 1996, Toronto, Canada, 1996:196.
[37] Mitsui H, Hosoi F, Ushirokawa M. J Appl Polym Sci 1975;19:361.
[38] Imai M. Radiat Phys Chem 1981;18 (3) 4:425.
[39] Fujimura T, Hayakawa N, Kuriyama I. J Appl Polym Sci 1982;27:4085.
[40] Fujimura T, Hayakawa N, Kuriyama I. J Appl Polym Sci 1982;27:4093.
[41] Ries M, Rose R, Greer J, Weaver K, Sauer W, Beals N. Sterilization induced effects on UHMWPE performance properties. In: Proceedings of the Orthopedic Research Society, 41st Annual Meeting, 13–16 February 1995, Orlando, FL, 1995:757.
[42] Reber E, Higgins J. Effects of gamma radiation on uniform compression molded and extruded polyethylene packaged in air and argon. In: Society of Biomaterials Transactions, 5–9 April 1994, Boston, MA, 1994:188.
[43] Tidjani A, Watanabe Y. J Polym Sci, Polym Chem Ed 1995;33:1455.
[44] Premnath V, Harris WH, Jasty M, Merrill E. Biomater 1996;17:1741.
[45] Malliaris A, Turner DT. J Polym Sci A-1 1971;9:1765.
[46] Jaworska E, Piskorz W. Radiat Phys Chem 1988;32 (5):715.
[47] Shaban AM, Kinawy N. Polymer 1995;36 (25):4767.
[48] Satula LC, Saum KA, Collier JP, Currier BH. Time dependent oxidation and damage in retrieved and never implanted UHMWPE

components. In: Proceedings of the Orthopaedic Research Society, 41st Annual Meeting, 13–16 February 1995, Orlando, FL, 1995:118.
[49] McKellop H, Yeom B, Campbell P, Salovey R. Radiation induced oxidation of machined or molded UHMWPE after seventeen years. In: Society of Biomaterials Transactions, 21st Annual Meeting, 18–22 March 1995, San Francisco, CA, 1995:54.
[50] Sun DC, Schmidig G, Stark C, Dumbleton JH. On the origins of a subsurface oxidation maximum and its relationship to the performance of UHMWPE implants. In: Society of Biomaterials Transactions, 21st Annual Meeting, 18–22 March 1995, San Francisco, CA, 1995:362.
[51] Trieu HH, Paxson RD. The oxidized surface layer in shelf-aged UHMWPE tibial inserts. In: Proceedings of the Orthopaedic Research Society, 41st Annual Meeting, 13–16 February 1995, Orlando, FL, 1995:758.
[52] Bostrom MPG, Bennet AP, Rimnac CM, Wright TM. Degradation in polyethylene as a result of sterilization, shelf storage, and in vivo use. In: Proceedings of the Orthopaedic Research Society, 40st Annual Meeting, 21–24 February 1994, New Orleans, LA, 1994:288.
[53] Bellare A, Cohen R. Biomater 1996;17:2325.
[54] Glatter O. J Appl Crystallogr 1977;10:415.
[55] Glatter O. Acta Phys Aust 1977;47:83.
[56] Glatter O, Hainish B. J Appl Crystallogr 1984;17:435.
[57] Tanabe Y, Strobl GR, Fischer EW. Polymer 1986;27:1147.
[59] Bellare A, Schnablegger H, Cohen RE. Macromolecules 1995;28:7585.
[60] Bhateja SK, Duerst RW, Aus EB, Andrews EH. J Macromol Sci Phys 1995;B34 (3):263.
[61] Oonishi S-I, Sugimoto S-I, Nitta I. Electron spin resonance study of radiation oxidation of polymers. IIIA. results for polyethylene and some general remarks. J Polym Sci Part A 1963;1:605.
[62] Wunderlich B. In: Turi EA, editors. Thermal characterization of polymeric materials, vol. 1, 2nd ed. San Diego, CA: Academic Press, San Diego, 1997:392.